

# Cooperative Hydrogen- and $\pi$ H-Bonded Interactions Involving Water and the Ethylenic Double Bond

Donald B. DuPré\* and M. Cecilia Yappert

Department of Chemistry, University of Louisville, Louisville, Kentucky 40292

Received: September 17, 2001; In Final Form: November 2, 2001

$\pi$ H-bonded complexes of water and the water dimer with ethene, propene, *trans*-2-butene, and allyl alcohol were examined in structures calculated ab initio at MP2/6-311++G(2d,2p). Cooperative enhancement of  $\pi$ H and  $\sigma$ H bonds is observed in the presence of hydroxy groups either from the second water or the alcohol. These interactions are analyzed in terms of structural changes, binding energies, normal-mode frequency shifts and intensity increases, and donor–acceptor charge transfers among local (natural bond) orbitals that nonadditively polarize participating bonds. The field effect of electron-releasing methyl groups attached to the double bond is also shown to strengthen the  $\pi$ H bond.

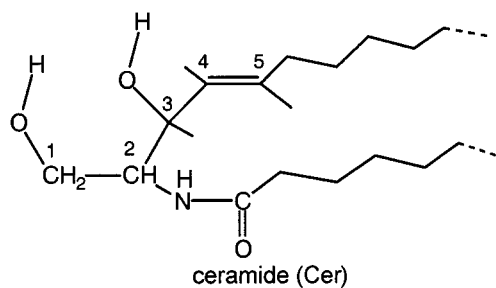
## Introduction

The sphingolipid metabolite ceramide (Cer) has been identified as an active lipid second messenger in the regulation of cell growth, differentiation, and apoptosis.<sup>1</sup> Its saturated analogue, dihydroceramide, lacks biological activity.<sup>2,3</sup> The critical, *trans*-double bond in the vicinity of the hydroxyl groups thus apparently imparts essential conformational features responsible for the physiological effects of Cer. Proton and <sup>13</sup>C NMR studies in our laboratory<sup>4</sup> indicate the presence of two tightly bound water molecules in this area of the monomeric lipid. Although extended application of a high vacuum is not sufficient to free these waters, they can be easily removed from dihydroceramide (without the double bond) and deoxydihydroceramide (without the OH group on C3). This observation, among others, suggests a unique, cooperative  $\pi$ H- and  $\sigma$ H-type hydrogen-bonded structural motif in Cer involving water and both of the lipid OHs, which may be important in the process of molecular recognition.

$\pi$ H-bonded complexes of water and the water dimer with ethene (and other larger alkenes and arenes) have been shown to exist in experimental studies of mixtures of these molecules in argon matrixes.<sup>5–9</sup> IR measurements<sup>5,6</sup> indicate that a water molecule will position itself with a  $H_\pi$  bond, involving only one of the OH groups, directed to the center of the double bond of ethene. The complex with two waters has both waters, hydrogen-bonded to one another, on the same side of the plane of ethene. Large red shifts in observed O–H stretching frequencies point to cooperative enhancement of both the  $\pi$ H bond and the  $\sigma$ H bond of the water dimer in the ternary complex. Microwave<sup>8</sup> and molecular beam<sup>7</sup> observations indicate that the water molecule in the  $H_2O \cdots$ ethene ( $W \cdots$ Eth) complex is in rapid rotation about the  $\pi$ -bonded axis, and the protons of water engage in quantum mechanical tunneling through a larger, bifurcated barrier in the plane of the water.

The nature of the weak,  $\pi$ -type hydrogen-bonding interaction has been studied theoretically, with an initial calculation of the  $W \cdots$ Eth complex by Del Bene.<sup>10</sup> More recent work, with extended basis sets and electron correlation, confirms the stability of ethene complexes with water.<sup>9,11–14</sup> Of

SCHEME 1: Ceramide



particular note is the enhancement of the strength of the  $\pi$ H bond caused by the presence of the second,  $\sigma$ -type hydrogen-bonded water in  $(H_2O)_2 \cdots$ ethene ( $W_2 \cdots$ Eth). The hydrogen bond across the water dimer is also strengthened by the presence of the  $\pi$ H bond in the complex. Thus, mutually enhancing, cooperative effects result from nonadditive redistributions of electrical charge among the monomers in these molecular clusters.

The purpose of this study was to further analyze cooperative bonding in complexes of ethene with water in terms of local bond orbital interactions. We also examined the field effect of methyl groups on the strength and cooperativity of the  $\pi$ H interaction with models of one and two water molecules interacting with propene and *trans*-2-butene. Finally, we extended the consideration to clusters involving the allyl alcohol (AOH) functionality that is a step closer to the situation in partially hydrated, membrane sphingolipids.

Our analysis makes use of natural bond orbital (NBO) theory.<sup>15–17</sup> The structural importance of  $\pi(C=C) \rightarrow \sigma^*(O-H_\pi)$  charge-transfer interactions is further demonstrated in two model complexes by removing this source of stabilization in the Fock matrix (thus “turning off” the  $\pi$ H bond) and reoptimizing the geometries.

## Computational Methods

To compute realistic interaction energies for weakly bound van der Waals (vdW) and hydrogen-bonded complexes, it is necessary to use flexible, extended basis sets with diffuse functions and to adequately account for electron correlation.<sup>9,18,19</sup>

\* Corresponding author. E-mail: d.dupre@louisville.edu.

Unfortunately, current density functional theory (DFT) functionals fail to reproduce important dispersion components for such complexes, and computationally more expensive methods of calculation such as Moller–Plesset perturbation theory (MPn) are required.<sup>18,20–22</sup> MPn past the second order seems to provide little additional benefit,<sup>18</sup> and thus MP2 is widely used in the study of hydrogen-bonding and vdW interactions.<sup>9,18</sup> At this level, the 6-311++G(2d,2p) basis set provides a feasible computational protocol for molecular clusters of moderate size. Some years ago,<sup>23</sup> the 6-311++G(2d,2p) basis set, of triple- $\zeta$  quality with diffuse and polarization functions on all atoms, was shown to achieve near Hartree–Fock limits in model hydrogen-bonded complexes. Coupled with MP2 calculations, this basis set yielded structures in good agreement with experiment.<sup>23</sup> More recently, MP2/6-311++G(2d,2p) and the related MP2/6-31++G(2d,2p) produced counterpoise corrected interaction energies for  $\text{H}_2\text{O}\cdots\text{CH}_4$ ,  $\text{H}_2\text{O}\cdots\text{C}_2\text{H}_4$ , and  $\text{H}_2\text{O}\cdots\text{C}_2\text{H}_2$  complexes that are remarkably close to the near Hartree–Fock basis set limit.<sup>12</sup> Reasonable correspondence with experimental electrostatic and induction properties of the constituent monomers also was found. Sorenson et al.<sup>24</sup> successfully applied MP2/6-311++G(2d,2p) to the study of the  $\text{H}_2\text{O}\cdots\text{benzene}$  complex, and Tsuzuki et al.<sup>19</sup> showed that 6-311++G(2d,2p) is almost saturated in the calculation of the interaction energy of the benzene dimer. We have thus used MP2/6-311++G(2d,2p) in all geometry optimizations and normal-mode analyses with routines available in the Gaussian 98 electronic structure package.<sup>25</sup> This level of theory and basis set is of similar quality to those used in recently reported<sup>9,11–14</sup> calculations on complexes of ethene with water and the water dimer.

Binding energies were calculated with the supermolecule approach as the difference,  $\Delta E$ , between the energy of the optimized complex and that of the monomers, in the geometry of the complex, with their local basis sets. Corrections were also made for the geometric deformation (def) of monomers as they are brought into the complex and zero-point vibrational energy (ZPVE). The problem of basis-set superposition error (BSSE) was dealt with a posteriori with the widely used counterpoise (CP) method of Boys and Bernardi,<sup>26</sup> to yield  $\Delta E_0(\text{CP}+\text{def}+\text{ZPVE})$ . The issue of BSSE is still controversial. At correlated levels, the standard CP correction has been shown to be an unreliable estimate of this error and produces unphysical increases in the virtual orbital space.<sup>27</sup> Kim et al.<sup>9</sup> suggested using only one-half of the CP correction to improve correspondence with experiment. Their rationale for this seemingly arbitrary percentage reduction is the recognition that basis-set incompleteness error is also present and is of the sign opposite to BSSE. Therefore, we also report  $\Delta E_0'(\text{CP}/2+\text{def}+\text{ZPVE})$  for the binding energy. Full harmonic ZPVE correction may also be an overestimate in weakly bound, vdW complexes with shallow potentials for intermolecular stretching and bending motion. Rovira et al.<sup>12</sup> suggested instead the use of the intermolecular stretching frequency for the dissociation of monomers in such complexes, calculated on the basis of a fitted, pseudodiatomic, and anharmonic Morse potential. This correction is much smaller than ZPVE and results, therefore, in stronger estimates of the binding energy. In all the complexes of our study, we are able to observe distinct (harmonic) intermolecular stretching modes involved in dissociation of molecules at the  $\pi\text{H}$  bond and, in the case of water dimers, also at the point of  $\text{C}-\text{H}\cdots\text{O}_w$  contacts with alkene hydrogens. We thus propose the use of these low-frequency vdW stretching modes (denoted  $S_2$ ) as an alternate, and easily obtained, correction for vibrational destabilization of these complexes.

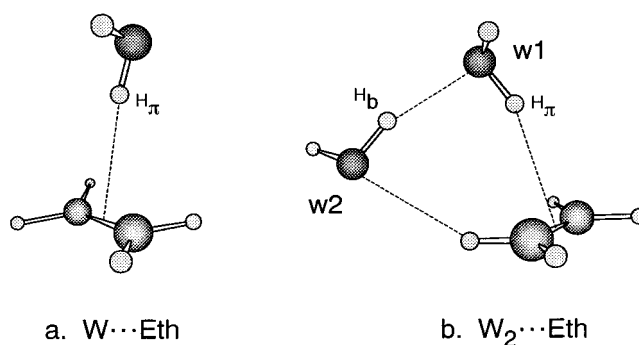


**Figure 1.**  $\pi\text{H}$ -bonded complexes of ethene with one and two water molecules. (a)  $\text{H}_2\text{O}\cdots\text{ethene}$  complex ( $\text{W}\cdots\text{Eth}$ ). (b) Complex with the water dimer ( $\text{W}_2\cdots\text{Eth}$ ). The  $\pi$ -bonded hydrogen is denoted  $\text{H}_\pi$ ; the hydrogen-bonded hydrogen,  $\text{H}_b$ . Free hydrogens are denoted  $\text{H}_f$  in the text. The two water molecules are distinguished as w1 and w2.

These numbers are also reported as  $\Delta E_0''(\text{CP}/2+\text{def}+\text{vdW})$  and give the strongest estimates of the binding energy.

NBO analysis performs the transformation of canonical molecular orbitals into an orthonormal set of one- and two-center localized orbitals (NBOs) analogous to traditional Lewis-type hybrid orbitals.<sup>15–17</sup> Sparsely occupied, nonideal antibonding and Rydberg orbitals also arise, which act as depositories of inter- and intramolecular electron charge transfers. The examination of these interactions is helpful in the study of the nature of donor–acceptor interactions, such as those that occur in hydrogen-bonded and vdW complexes. In this study, we refer to the  $\pi(\text{C}=\text{C})\rightarrow\sigma^*(\text{O}-\text{H}_\pi)$  interaction associated with the  $\pi\text{H}$  bond and the water oxygen lone pair  $n_p(\text{O})\rightarrow\sigma^*(\text{O}-\text{H})$  interaction involved in the  $\sigma\text{H}$  bond between water molecules or between water and the  $\text{O}-\text{H}_a$  of AOH. It is possible to estimate the energy lowering,  $E^{(2)}$ , caused by specific electron delocalizations with second-order perturbation theory.  $E^{(2)}$  is given by  $-2 \langle a|F|b\rangle^2/(E_a - E_b)$ , where  $\langle a|F|b\rangle$  is the matrix element of the effective one-electron Hamiltonian (Fock or Kohn–Sham matrix in the DFT) connecting two NBOs  $a$  and  $b$  of energy  $E_a$  and  $E_b$ . For this purpose, we used the B3LYP/6-311++G-(2d,2p) density calculated on respective MP2/6-311++G-(2d,2p)-optimized geometries. Even though direct aspects of dispersion are absent in these DFT wavefunctions, some measure of electron correlation is recovered in the interaction of NBOs and charges on atomic sites determined by natural population analysis (NPA). The geometries of two  $\pi\text{H}$ -bonded models,  $\text{W}\cdots\text{Eth}$  and  $\text{H}_2\text{O}\cdots\text{AOH}$  ( $\text{W}\cdots\text{AOH}$ ), were also reoptimized at the HF/6-31G\*\* level with the elimination of the elements in the Fock matrix that correspond to the  $\pi(\text{C}=\text{C})\rightarrow\sigma^*(\text{O}-\text{H}_\pi)$  and  $\sigma(\text{O}-\text{H}_\pi)\rightarrow\pi^*(\text{C}=\text{C})$  interactions.<sup>28</sup> Numerical Fletcher–Powell or eigenvalue following optimization routines in Gaussian 98 were used for this purpose.<sup>25</sup> NBO results are also advantageous in that they are unaffected by the presence of diffuse functions in the basis set.<sup>15</sup>

## Results and Discussion

The fully optimized geometries of  $\text{H}_2\text{O}\cdots\text{ethene}$  ( $\text{W}\cdots\text{Eth}$ ) and  $(\text{H}_2\text{O})_2\cdots\text{ethene}$  ( $\text{W}_2\cdots\text{Eth}$ ) are presented in Figure 1. The  $\pi$ -bonded water is denoted as w1, and the hydrogen-bonded water is distinguished as w2. We have also investigated complexes of one ( $\text{W}\cdots\text{AOH}$ )- and two-water ( $\text{W}_2\cdots\text{AOH}$ ) molecules with the AOH functionality, shown in Figure 2. Here one of the water molecules is tethered to the double bond and influenced by hydrogen-bonding to the alcohol functionality and by conformational constraints of  $-\text{CH}_2\text{OH}_a$  with respect to  $>\text{C}=\text{C}<$  in AOH. The field effect<sup>29</sup> of methyl groups on  $\pi\text{H}$ -

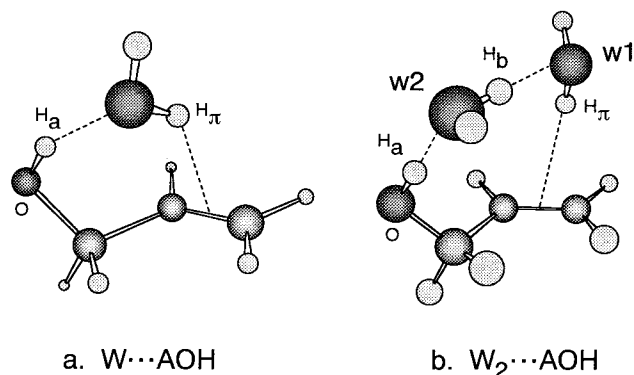


**Figure 2.**  $\pi$ H-bonded complexes of AOH with one and two water molecules. (a)  $W \cdots AOH$ ; (b)  $W_2 \cdots AOH$ . The hydrogen of the alcohol hydroxyl group is denoted  $H_a$ .

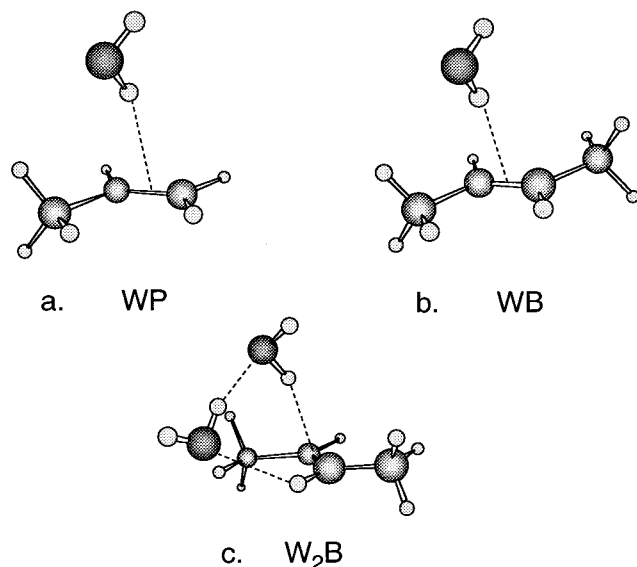


**Figure 3.** Influence of methyl group field effects on the  $\pi$ H bond. (a)  $H_2O \cdots$ propene (WP); (b)  $H_2O \cdots$ *trans*-2-butene (WB); (c)  $(H_2O)_2 \cdots$ *trans*-2-butene ( $W_2B$ ).

bond strength and cooperativity was studied with models of  $H_2O \cdots$ propene (WP),  $H_2O \cdots$ *trans*-2-butene (WB), and  $(H_2O)_2 \cdots$ *trans*-2-butene ( $W_2B$ ), shown in Figure 3. As a demonstration of the structural importance of the  $\pi(C=C) \rightarrow \sigma^*(O-H_\pi)$  charge-transfer interaction in these  $\pi$ H-bonded complexes, this source of stabilization was removed, along with the weaker  $\sigma(O-H_\pi) \rightarrow \sigma^*(C=C)$  interaction, in two model complexes,  $W \cdots Eth$  and  $W \cdots AOH$ , and the geometries reoptimized at the Hartree–Fock level.

**Geometric Parameters.** Some of the important structural parameters of water (W) and water dimer ( $W_2$ ) complexes with ethene and AOH are shown in Table 1. These geometries result from full ab initio optimizations at the MP2/6-311++G-(2d,2p) level, and correspond to stationary states on the potential energy surface with no imaginary normal-mode frequencies. Parameters for isolated W,  $W_2$ , and ethene at the same level of theory are also presented for comparison.

The structure of the  $\pi$ H-bonded complex of a single water with ethene ( $W \cdots Eth$ ) is shown in Figure 1a. The water molecule lies in a plane bisecting the double bond with one of the hydrogens,  $H_\pi$ , pointing directly toward and bonding with the  $\pi$ -electronic structure. The oxygen atom is tilted to one side so that the other hydrogen,  $H_f$ , although not  $\pi$ H-bonded, also lies above the double bond. The distance of  $H_\pi$  to the center of  $>C=C<$ , denoted here as  $H_\pi \cdots ||$ , is calculated to be 2.394 Å,

**TABLE 1: Geometric Parameters Calculated at MP2/6-311++G(2d,2p) for Monomers and Hydrogen- and  $\pi$ H-Bonded Complexes of Water (W) with Ethene (Eth) and the AOH Moiety<sup>a</sup>**

geometric parameters	$H_2O$	$(H_2O)_2$	$W \cdots Eth$	$W_2 \cdots Eth$	$W \cdots AOH$	$W_2 \cdots AOH$
w1 O– $H_\pi$	0.958	0.959	0.962	0.965	0.964	0.967
O– $H_f$	0.958	0.959	0.958	0.959	0.959	0.959
$\angle H_2O$	104.2°	104.7°	104.4°	105.0°	105.4°	105.0°
w2 O– $H_b$		0.965		0.967		0.971
O– $H_f$		0.957		0.957		0.958
$\angle H_2O$		104.6°		105.0°		106.0°
$H_b \cdots O$		1.956		1.929		1.847
$\angle O-H_b \cdots O$		172.4°		162.0°		163.6°
$H_a \cdots O$					1.980	1.851
O– $H_a$					0.966	0.970
$\angle COH_a$					106.4°	108.0°
$\angle O-H_a \cdots O$					154.8°	176.2°
C=C	1.334		1.336	1.337	1.339	1.339
$H_\pi \cdots   $			2.394	2.341	2.417	2.313

<sup>a</sup> The water dimer is denoted  $W_2$ . w1 is the free, proton acceptor or  $\pi$ H-bonded water. w2 is the proton donor water in the water dimer.  $H_a$  is the proton on the alcohol functionality. The  $\pi$ H-bonded hydrogen is indicated by  $H_\pi$ , the hydrogen-bonded hydrogen by  $H_b$ , and free hydrogens by  $H_f$ .  $H_\pi \cdots ||$  is the distance of  $H_\pi$  to the center of mass of the double bond ( $C=C$ ). Distances are in angstroms; angles are in degrees.

which compares with the experimental value of 2.482 Å measured for this complex in argon expansions by molecular beam electric resonance spectroscopy.<sup>7</sup> It is also noteworthy that the O– $H_\pi$  and C=C distances lengthen slightly in the complex. As will be discussed further below, the weakening of these bonds is a consequence of the intermolecular  $\pi(C=C) \rightarrow \sigma^*(O-H_\pi)$  charge-transfer interaction between the respective local (natural) bonds. This depletes the bonding electron occupancy of  $\pi(C=C)$  and adds electron density to the antibonding orbital of O– $H_\pi$ , thus weakening both bonds.

The addition of another water (w2) to form the  $W_2 \cdots Eth$  complex of Figure 1b results, not unexpectedly, in a hydrogen-bonded water dimer clustering on one side of the  $\sigma$ -bonded plane of ethene. As seen in the bond distances of Table 1, both the  $\pi$ H bond and the hydrogen bond of  $W_2$  are strengthened in the complex. The  $\pi$ H-bond distance,  $H_\pi \cdots ||$ , is reduced by  $\sim 0.05$  Å (compared with  $W \cdots Eth$ ) and the hydrogen-bond distance,  $H_b \cdots O_{w1}$ , is reduced by  $\sim 0.03$  Å (compared with the isolated water dimer) in the complex. This is the first evidence of cooperative bonding effects, discussed below in terms of electron delocalization and nonadditive bond polarizations over the entire complex. The oxygen of w2 is also found to be engaged in a weak interaction with one of the C–H bonds of ethene, and the array is thus statically cyclic. Such C–H $\cdots$ O hydrogen bonds, albeit weak, have been shown to exist and have been studied experimentally and theoretically.<sup>30–32</sup>

The complexes of water with the AOH moiety (Figure 2) are more closely related to hydration of the polar region of ceramide and sphingomyelin. A single water molecule is preferentially hydrogen-bonded to the O– $H_a$  functionality and tethered to the double bond as in Figure 2a. As measured by gross geometric parameters (bond distance and O– $H_a \cdots O_w$  bond angle), the  $H_a \cdots O_w$  hydrogen bond is weaker here than in the water dimer, either in isolation or in the  $W_2 \cdots Eth$  complex. The  $\pi$ H bond is also weaker, with  $H_\pi \cdots ||$  rising to 2.417 Å. Inspection of the geometry of  $W \cdots AOH$  shows that the water molecule, although bonded with the  $\pi$ -electron structure of the double bond, is pulled off the optimal site at the center of  $>C=C<$  by the constraints of the  $\sigma$ -bonded framework and dihedral angles of the AOH substrate. In  $W_2 \cdots AOH$  (Figure

**TABLE 2: Energies in kilocalories per mole calculated at MP2/6-311++G(2d,2p)<sup>a</sup>**

	(H <sub>2</sub> O) <sub>2</sub>	W⋯Eth	W <sub>2</sub> ⋯Eth		W⋯AOH	W <sub>2</sub> ⋯AOH	
			→2W+π	→W <sub>2</sub> +π		→2W+π	→W <sub>2</sub> +π
ΔE	-5.40	-2.86	-10.14	-4.90	-7.07	-16.20	-11.02
% correlation	27.6	70.2	47.8	68.5	54.5	42.0	48.3
corrections							
BSSE(CP)	0.91	0.57	1.77	0.86	1.35	2.93	1.90
deformation	0.04	0.01	0.12	0.25	0.26	1.18	1.35
ZPVE	2.23	1.28	3.68	1.46	1.99	4.29	2.06
vdW	0.51	0.16	0.38	0.38	0.45	0.47	0.47
ΔE <sub>0</sub> (CP+def+ZPVE)	-2.22	-0.99	-4.56	-2.34	-3.47	-7.80	-5.71
ΔE <sub>0</sub> ' (CP/2+def+ZPVE)	-2.68	-1.28	-5.45	-2.77	-4.14	-9.27	-6.66
ΔE <sub>0</sub> " (CP/2+def+vdW)	-4.39	-2.40	-8.75	-3.85	-5.69	-13.09	-8.25
ΔE <sub>dissoc</sub> (expt. est.) <sup>b</sup>		-2.4 ± 0.5	-8 to -7.5	-3.6			
E <sup>(2)</sup> (NBO)							
n <sub>p</sub> (O <sub>w1</sub> )→σ*(O-H <sub>b</sub> )	7.07			7.86		11.43	
n <sub>p</sub> (O <sub>w1</sub> )→σ*(O-H <sub>alc</sub> )					6.55		
n <sub>p</sub> (O <sub>w2</sub> )→σ*(C-H)				0.84			
n <sub>p</sub> (O <sub>w2</sub> )→σ*(O-H <sub>alc</sub> )						11.38	
π(C=C)→σ*(O-H <sub>π</sub> )		2.48		3.25	2.14	4.27	
NPA charges							
w1	13.82	-5.12		7.42	8.30	12.65	
w2	-13.82			-13.76		-0.10	
alkene		5.12		6.36	-8.30	-12.55	

<sup>a</sup> Two monomeric water molecules are indicated by 2W, whereas the water dimer is denoted W<sub>2</sub>. Two modes of dissociation, to isolated monomers (→2W+π) or to the water dimer and alkene (→W<sub>2</sub>+π), are shown for complexes involving W<sub>2</sub>. NPA charges (in millielectrons) and NBO second-order perturbation energies, E<sup>(2)</sup>, determined with B3LYP densities. BSSE is corrected for by the CP method, either in full or 50%. An alternative to full-harmonic, ZPVE correction is the zero-point vibrational energy of just the vdW mode(s) that result in a pulling apart of the complex.

<sup>b</sup> Engdahl and Nelander.<sup>5,6</sup> expt. est., experimental estimate.

2b), however, more orientational flexibility exists, and the water dimer fits more effectively between the double bond and O-H<sub>a</sub>. Geometric parameters of W<sub>2</sub>⋯AOH suggest that both the πH bond and the hydrogen bond are further enhanced. The H<sub>a</sub>⋯O<sub>w2</sub> and H<sub>b</sub>⋯O<sub>w1</sub> hydrogen-bond distances are both about 1.85 Å and H<sub>π</sub>⋯|| is further reduced to 2.313 Å. Thus, in the W<sub>2</sub>⋯AOH complex, the πH-bond H<sub>π</sub>⋯|| distance has decreased by ~0.1 Å, as compared with W⋯Eth; the hydrogen bond of w2 with the alcohol is stronger than that of the water dimer; and the hydrogen-bond distance (though not angle) in W<sub>2</sub> has been enhanced relative to the isolated water dimer. The further lengthening of C=C, O-H<sub>π</sub>, O-H<sub>b</sub>, and O-H<sub>a</sub> should also be noted, because these are gross physical consequences of local bond/antibond donor-acceptor interactions accounted for in some theories of the formation of the hydrogen bond<sup>15-17</sup> and, here, of the πH bond.

Geometric parameters alone are not definitive in terms of assessment of hydrogen-bond or vdW complexation strengths. Measures of other factors, such as binding energies and inter- and intramolecular charge redistributions, must also be consulted.

**Binding Energies.** The results of our calculations on the binding energy of water and the water dimer to the above πH-bonded complexes are presented in Table 2. Values for the isolated water dimer are also listed for comparison. It is seen that 42–70% of the uncorrected ΔE of the π-bonded complexes is caused by correlation effects, as measured by the difference in the MP2 and Hartree-Fock energies. This effect is more important for the πH-bonding component as seen in differences in ΔE between the paths of separation of the water dimer and both individual waters from the alkene. Correlation is also less important for the calculation of the dissociation energy of the isolated water dimer itself. BSSE is lower for the complexes with ethene than for those with AOH, being smaller in each category for those that dissociate without the breakup of the water dimer. The deformation energy is trivial, except in W<sub>2</sub>⋯AOH where the AOH component undergoes a more

significant change in geometry in the formation of the complex. The ZPVE correction is the greatest destabilization factor in these complexes (and in the isolated water dimer). If this factor is reduced with the correction discussed above involving intermolecular vdW stretching mode(s), the calculated results agree almost exactly with experiment. Whatever the most appropriate set of corrections might be, the πH bond is enhanced significantly by the presence of the hydrogen bond to a second water molecule and/or to the allylic alcohol. ΔE approximately doubles in going from W⋯Eth to W<sub>2</sub>⋯Eth, as measured in the latter case by the dissociation to the water dimer. The addition of the allylic alcohol hydrogen bond is responsible for another doubling of the binding energy in going from W<sub>2</sub>⋯Eth to W<sub>2</sub>⋯AOH. From these calculations, we estimate an upper bound on the binding energy of two water molecules to the AOH substrate of ceramide to be 8 to 13 kcal/mol depending on the mode of dissociation (single water molecules breaking off or the removal of the intact water dimer). This is two to three times the accepted value for the dissociation of the water dimer in the gas phase and should be structurally significant as indicated by our previous experiments<sup>4</sup> with ceramide analogues, where it is difficult to remove two adventitious water molecules held in the vicinity of the AOH functionality.

**Local Bond (NBO) Analysis of Donor-Acceptor Interactions.** NBO theory attributes A-H⋯B hydrogen-bond formation to donor-acceptor interactions of local bonds, where a lone pair on the base, n(B:), transfers charge into an antibonding σ\*(A-H) orbital on the acid.<sup>15-17</sup> In terms of the water dimer, for example, it is the n<sub>p</sub>(O<sub>w1</sub>)→σ\*(O<sub>w2</sub>-H<sub>b</sub>) interaction that overcomes enough of the intermolecular exchange repulsion to draw the molecules together within the vdW contact surfaces of H<sub>b</sub> and O<sub>w1</sub>. For the πH bond, π(C=C)→σ\*(O-H<sub>π</sub>), involving the π-electron density of the slightly basic double bond, would be the operative interaction. Even small amounts of electron delocalization by such mechanisms can be chemically significant, with 10 me corresponding to ~6 kcal/mol stabilization.<sup>15</sup> The effect of dispersion<sup>16</sup> reduces repulsions and enhances

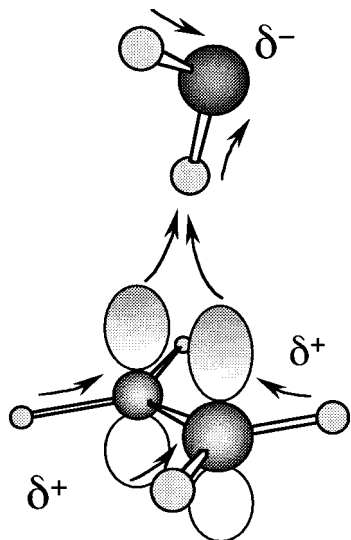


**Figure 4.** Charge redistribution in the  $W\cdots Eth$  complex. Overall, negative charge flows from the tails of the base (hydrogens of ethene) to the head of the acid (oxygen of water). More charge is redistributed on the formation of the  $\pi H$  bond within, rather than between, the molecules.

bond/antibond donor–acceptor interactions already present at the uncorrelated self-consistent field level. For methods where an effective one-electron Hamiltonian is available, a measure of the relative strength of donor–acceptor charge-transfer interactions is found in the relative value of  $E^{(2)}$  obtained from second-order perturbation theory. These values, calculated with the use of the DFT (here B3LYP) density, are also presented in Table 2. It is seen that the  $\pi H$ -bond interaction in  $W\cdots Eth$  is less than half as strong as that of the  $\sigma H$ -bonded water dimer (2.48 vs 7.07 kcal/mol). For  $W_2\cdots Eth$ , this interaction increases by about 30% and the hydrogen-bond interaction of the water dimer is also enhanced by  $\sim 11\%$ . In other terms, the  $\pi H$  and  $\sigma H$  bonds cooperatively enhance one another in the complex, albeit to different extents. A smaller  $n_p(O_{w2})\rightarrow\sigma^*(C-H)$  interaction arising from a  $C-H\cdots O_w$  hydrogen bond with the  $\sigma$ -bonding framework of ethene is also noted.

The association of one water with the AOH moiety is stabilized by a hydrogen bond to the alcohol and a weaker  $\pi H$  bond, with  $\pi(C=C)\rightarrow\sigma^*(O-H_\pi)$  falling to 2.14 kcal/mol ( $W\cdots AOH$ ). The strongest complex is that with two waters,  $W_2\cdots AOH$ , where the monomers have greater steric flexibility to complete a cycle of cooperative donor–acceptor charge transfers. The value of  $E^{(2)}$  for the  $\pi H$ -bonding interaction increases to 4.27 kcal/mol, which is 70% and 100% more, respectively, than that found for  $W\cdots Eth$  and  $W\cdots AOH$ . A similar  $\sim 70\%$  percentage increase, relative to the water dimer and to  $W\cdots AOH$ , occurs in the  $\sigma H$  bonds, where  $E^{(2)} = 11.4$  kcal/mol.

The origin of these cooperative effects can be traced by examining charges from natural population analysis and bond polarizations within the complexes. On the formation of the  $\pi H$  and the  $\sigma H$  bonds, it is generally found that negative charge flows from the regions of the base (tails of the base) remote from negative charge concentration to the region of the acid (head of the acid) close to negative charge concentration. This is illustrated in Figure 4 for the  $W\cdots Eth$  complex. More charge is redistributed within each monomer than is transferred between or among monomers of a complex. The electron density of the hydrogen atoms (tails of the base) and the double bond of ethene that is transferred to water in the  $W\cdots Eth$  complex resides

mostly on the oxygen atom that has a charge of  $-0.937$  e, as compared with  $-0.926$  e calculated for an isolated water molecule. The bonded hydrogen,  $H_\pi$ , is more positive ( $+0.473$  e) than the free hydrogen in the complex ( $+0.459$  e) or in the isolated water molecule ( $+0.463$  e). The increase in charge on the oxygen atom makes this site more susceptible to additional hydrogen bonding as occurs in the  $W_2\cdots Eth$  complex. In that case, the charge on  $H_\pi$  increases further to  $+0.488$  e, with that on  $O_{w1}$  rising to  $-0.952$  e. The oxygen on the proton donor,  $w_2$ , is the most negative ( $-0.963$  e), making it even more capable of further networking. This occurs to the maximal extent in our studies with  $W_2\cdots AOH$ , where the charge on  $H_\pi$  rises to  $+0.491$  e; that on  $H_b$ , to  $+0.499$  e; and that on  $H_a$ , to  $+0.497$  e. The latter value should be compared with  $+0.457$  e found for the charge on  $H_a$  in isolated AOH. The charges on the respective oxygen atoms are also the greatest in  $W_2\cdots AOH$ , with  $O_{w1}$  at  $-0.953$  e,  $O_{w2}$  at  $-0.970$  e, and  $O_a$  at  $-0.764$  e. The polarization of the proton donor bonds are thus all mutually enhanced through the cycle of cooperative charge-transfer interactions mapped by NBO analysis.

Further evidence of the  $\pi H$ -bond interaction is found in the examination of natural localized molecular orbitals. The natural localized molecular orbital dominated by  $\pi(C=C)$  has a delocalization tail into  $O-H_\pi$ , which progressively increases in going from  $W\cdots Eth$  (0.40%) to  $W_2\cdots Eth$  (0.57%) to  $W_2\cdots AOH$  (0.71%).

**Vibrational Frequencies and vdW Modes involving the  $\pi H$  Bond.** The results of the harmonic, normal-mode frequency analyses are shown in Table 3. Of particular interest are the red shifts and IR intensity increases found for the  $\bar{\nu}_s(O-H)$  symmetric stretching modes as the level of  $\sigma H$ - and  $\pi H$ -bonding increases. With the monomers and the water dimer as a reference, these experimentally observable parameters also exhibit substantial, sometimes dramatic, changes that are indicative of the cooperative effects considered above. For example,  $\bar{\nu}_s(O-H)$  of the  $\pi$ -bonded water in  $W\cdots Eth$  undergoes a calculated 45  $cm^{-1}$  red shift and a 13-fold IR intensity increase, relative to an isolated water molecule. This effect for the  $\pi$ -bonded water is about doubled in the complex of ethene with the water dimer. In  $W_2\cdots Eth$ ,  $\bar{\nu}_s(O-H)$  for the hydrogen-bonded water ( $w_2$ ) is even more substantially red shifted by 137.4  $cm^{-1}$  with a similar 25-fold increase in IR intensity, as compared with an isolated water molecule. Some experimental data, also presented in Table 3, are available<sup>5,6</sup> for these species which confirm the calculated relative, although not absolute, values of the red shifts in  $\bar{\nu}_s(O-H)$  of  $W\cdots Eth$  and  $W_2\cdots Eth$ . Again, and bearing on the issue of donor–acceptor cooperative effects, the shift ( $-120.0$   $cm^{-1}$ ) and intensity increase (33-fold) of  $\bar{\nu}_s(O-H_\pi)$  calculated for  $w_1$  in  $W_2\cdots AOH$  are the greatest found in our study. The symmetric O–H stretching mode of  $w_2$  in this compound is not individually isolable, for comparison, because it is strongly coupled with symmetric stretching vibrations of the other bonded O–H groups.

Changes in the symmetric  $\nu_7$  out-of-plane C–H bending mode of ethene and the symmetric intermolecular vdW stretching mode  $S_z$  are noteworthy. Both modes are blue shifted as bonding in the complexes increases, but little change occurs in IR intensity. The  $\nu_7$  mode of ethene is thought<sup>5</sup> to be associated with exchange repulsion between the  $\pi$ -orbital and the electron density on water and was used in the experimental estimation<sup>5</sup> of the binding energy of  $W\cdots Eth$  and  $W_2\cdots Eth$  (values reproduced in our Table 2). The  $S_z$  vdW mode should be related to the dissociation of the complex<sup>13,14</sup> because it involves a pulling away (and return) of the monomers with little or no

**TABLE 3: Harmonic Frequency Analysis of Normal Modes of Vibration Calculated at MP2/6-311++G(2d,2p)<sup>a</sup>**

	reference monomers	(H <sub>2</sub> O) <sub>2</sub>	W··Eth	W <sub>2</sub> ··Eth	W··AOH	W <sub>2</sub> ··AOH
w1 sym. str.	3861.4 (10)	-9.5 (1.5)	-45.0 (13)	-86.8 (23)	-66.6 (16)	-120.0 (33)
asym. str.	3981.3 (73)	-13.3 (1.3)	-26.8 (2)	-45.8 (2.0)	-42.3 (1.9)	-55.3 (2.1)
w1 sym. str. (expt.)	3638.0		-25.0	-51.8		
asym. str. (expt.)	3734.3		-16.8			
w2 sym. str.		-94.4 (29)		-137.4 (25)		
asym. str.		-30.4 (1.5)		-37.1 (1.4)		-42.8 (1.4)
w2 sym. str. (expt.)				-92.9		
ethene <i>v</i> <sub>7</sub> mode	970.3 (98.8)		14.5 (1.1)	32.0 (1.0)		
<i>v</i> <sub>7</sub> (expt.)	947.3		12.2	20.6		
S <sub>z</sub> vdW mode(s) <sup>b</sup>			108.7 (0.6)	123.1 (1.8)	π 132.0 (4.7) h 185.1 (13.2)	π 126.3 (0.8) π/h 147.5 (2.3) h 204.0 (6.9)

<sup>a</sup> Absolute values of frequencies in cm<sup>-1</sup> (and IR intensity in km/mol) are listed for the reference monomers and intermolecular vdW, S<sub>z</sub> stretching modes. Shifts (and IR intensity ratio) relative to reference monomer are given for the molecular complexes. Note that the stretching frequencies of water are red-shifted upon complexation and IR intensities are increased, sometimes substantially. Frequencies of the ethene *v*<sub>7</sub> out-of-plane bending mode and the S<sub>z</sub> modes are blue-shifted in the complexes. Experimental frequency shifts are from the studies of Engdahl and Nelander.<sup>5,6</sup> sym., symmetrical; str., stretching; asym., asymmetrical; expt., experimental. <sup>b</sup> π, h indicates dissociation from the πH or hydrogen bond. The three modes listed for W<sub>2</sub>··AOH clearly involve the dissociation of the intact water dimer from AOH, with W<sub>2</sub> pulling away in one-half cycle from the OH hydrogen bond (204.0), the πH bond (126.3), or alternately from both (147.5). The empirical scaling factor for calculated high-frequency vibrations of the water molecule is 0.940.

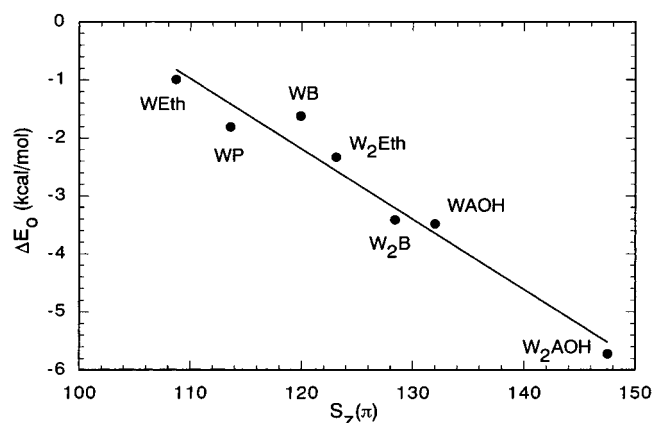


**Figure 5.** Correlation of the calculated symmetric vdW stretching mode, S<sub>z</sub>(π) (in cm<sup>-1</sup>), with the ΔE<sub>0</sub>(CP+def+ZPVE) binding energy (in kcal/mol) of the series of π-bonded complexes studied here. The value of the S<sub>z</sub>(π/h) mode is plotted for W<sub>2</sub>··AOH. The straight line is a linear least-squares fit with correlation coefficient, R = 0.98.

intramolecular distortions. Intermolecular, S<sub>z</sub>-type dissociation modes are evident in the AOH analogues not only for the πH

bond, denoted S<sub>z</sub>(π), but also for the normal hydrogen bonds, denoted S<sub>z</sub>(h). It may be possible to resolve experimentally the predicted values and trends in S<sub>z</sub> in cryospectroscopic measurements in the mid-IR. Here the modes may appear as hot bands on the high-frequency side of the more intense and noninterfering, symmetric O–H stretching mode of the bound water.<sup>33,34</sup> Even if the mode cannot be observed easily, it has theoretical significance. For example, a correlation is noted in Figure 5 between S<sub>z</sub>(π) and the binding energy of the πH complexes studied here. The plot shown is based on the fully corrected ΔE<sub>0</sub>(CP+def+ZPVE) and includes points for water associations with propene and *trans*-2-butene to be discussed below in relation to the field effect of the methyl group on the strength of the πH bond.

**The Field Effect of Methyl Group Substituents.** The possible electron-releasing, field effect<sup>29</sup> of methyl group substituents on the double bond, and subsequent strengthening of the πH bond, was examined with ab initio calculations on the propene and *trans*-2-butene derivatives in complexes WP, WB, and W<sub>2</sub>B shown in Figure 3. Essential geometric, charge-transfer, and energetic factors are summarized in Table 4 and compared with the analogous complexes with ethene.

**TABLE 4: Important Structural and Energetic Parameters for the Field Effect of Methyl Groups on the πH-Bond Interaction with W and W<sub>2</sub><sup>a</sup>**

	W··Eth	W··propene(WP)	W··butene(WB)	W <sub>2</sub> ··Eth	W <sub>2</sub> ··butene(W <sub>2</sub> B)
w1 OH <sub>τ</sub>	0.962	0.963	0.964	0.965	0.968
w2 OH <sub>b</sub>				0.967	0.967
H <sub>b</sub> ··O <sub>w1</sub>				1.929	1.931
H <sub>τ</sub> ··	2.394	2.343	2.290	2.341	2.226
ΔE (uncorrected)	-2.86	-3.76	-4.08	-4.90	-6.59
ΔE <sub>0</sub> (CP+def+ZPVE)	-0.99	-1.62	-1.81	-2.34	-3.41
ΔE <sub>0</sub> ' (CP/2+def+ZPVE)	-1.28	-2.02	-2.30	-2.77	-4.13
ΔE <sub>0</sub> '' (CP/2+def+vdW)	-2.40	-3.16	-3.39	-3.85	-5.23
ΔE <sub>dissoc</sub> (expt. est) <sup>b</sup>	-2.4 ± 0.5	-3.2 ± 0.6	-3.7 ± 0.7		
E <sup>(2)</sup> n <sub>p</sub> (O <sub>w1</sub> )→σ*(O–H <sub>b</sub> )				7.86	7.78
n <sub>p</sub> (O <sub>w2</sub> )→σ*(C–H)				0.84	0.11, 0.03
π(C=C)→σ*(O–H <sub>τ</sub> )	2.48	2.79	3.28	3.25	4.54
NPA charges: w1	-5.12	-6.21	-6.73	7.42	4.59
w2				-13.76	-13.62
alkene	5.12	6.21	6.73	6.36	9.04

<sup>a</sup> Geometric and bonding energy calculations performed at MP2/6-311++G(2d,2p). NPA charges (in millielectrons) and NBO second-order perturbation energies, E<sup>(2)</sup>, determined for these geometries with the B3LYP density. Only binding energy values (in kcal/mol) for dissociation to the water dimer are shown for W<sub>2</sub> complexes. Values for the respective complexes with ethene are included for ease of comparison. <sup>b</sup> Engdahl and Nelander.<sup>5,6</sup>

The methyl group indeed enhances the strength of the  $\pi$ H-bonded interaction. The distance of  $H_{\pi}$  of the water from the center of the double bond decreases in going from  $W \cdots \text{Eth}$  to  $WP$  to  $WB$ , 2.394 Å to 2.343 Å to 2.290 Å, respectively. The  $\pi$ H bond to the water dimer also becomes stronger when  $W_2 \cdots \text{Eth}$  is methylated to become  $W_2B$ , as seen in the decrease of the  $H_{\pi} \cdots ||$  distance from 2.341 to 2.226 Å. Calculated values of the vdW corrected binding energy compare well with available experimental estimates,<sup>6</sup> also presented in Table 4, for  $WP$  and  $WB$ . NBO analysis shows corresponding increases in  $E^{(2)}$  for the  $\pi(C=C) \rightarrow \sigma^*(O-H_{\pi})$  interaction, the highest value being for  $W_2B$ , which is 64% of that found at the same level of theory for the water dimer. Monitoring the flow of NPA calculated charge in these complexes reveals that most of the charge transferred to the  $\pi$ -bonded water comes from the out-of-plane hydrogens of the methyl groups that are oriented to hyperconjugate with the  $\pi$ -electron density of the double bond. This observation is consistent with the field effect and hyperconjugative  $+M$  mesomeric effect of an electron-releasing methyl moiety. Indeed, NBO analysis also demonstrates that more charge is transferred by hyperconjugative pathways from out-of-plane methyl  $\sigma(C-H)$  bonds into  $\pi^*(C=C)$  of the double bond than from  $\pi(C=C)$  into the corresponding  $\sigma^*(C-H)$  antibonds.

On the basis of the vdW-corrected  $\Delta E_0$ , which are closest to experimentally known values of the binding energy, the field effect of adding two methyl groups to the double bond of ethene is approximately 75% of that associated with the increase of the  $\pi$ H bond due to cooperative  $\sigma$ H bonding with an additional water molecule. The values of  $E^{(2)}$  for the  $\pi(C=C) \rightarrow \sigma^*(O-H_{\pi})$  interaction, however, are approximately the same for the two effects in these two cases. The geometric effect in drawing the  $\pi$ H-bonded water to the double bond is the same for one methyl group (in  $WP$ ) as for the cooperative effect that occurs on the addition of another  $\sigma$ H-bonded water (in  $W_2 \cdots \text{Eth}$ ). Two methyl group substituents in  $W_2B$  decrease this distance even further than that found for the cyclic  $W_2 \cdots \text{AOH}$  complex.

**Turning Off the  $\pi$ H Bond.** An experiment is possible in the context of NBO theory where specific interaction elements of the Fock matrix are set to zero and the geometry of the molecule, or here molecular cluster, is reoptimized.<sup>15,17</sup> The procedure illustrates the influence of the donor–acceptor mode or modes in question on manifest features of molecular structure. We have used this method to “turn off” the  $\pi$ H bond in models of  $W \cdots \text{Eth}$  and  $W \cdots \text{AOH}$ . These calculations are time-consuming, and thus necessitate the use of a less extensive basis set and the Hartree–Fock level of theory. The effects are, however, recovered in the results. Without the possibility of electron delocalization due to  $\pi(C=C) \rightarrow \sigma^*(O-H_{\pi})$  and  $\sigma(O-H_{\pi}) \rightarrow \pi^*(C=C)$ , the water molecule of  $W \cdots \text{Eth}$  was found to drift away from ethene, with a change of  $H_{\pi} \cdots ||$  from 2.687 to 3.235 Å, when calculated at the HF/6-31G\*\* level. When the  $\pi$ H bond was turned off in the  $W \cdots \text{AOH}$  complex,  $H_{\pi} \cdots ||$  increased from 2.730 to 3.235 Å, also calculated at the HF/6-31G\*\* level. This allowed the water molecule to approach the alcohol functionality of AOH more closely and the hydrogen-bond distance  $H_a \cdots O$  decreased from 2.057 Å, when  $\pi$ -bonding was active, to 2.031 Å in its absence.

## Conclusions

This work demonstrates and quantifies the strength of the  $\pi$ H-type hydrogen bond between a single water molecule and the double bond of ethene. Furthermore, the results highlight

the cooperative enhancement of this interaction in the presence of more water molecules and/or the hydroxyl group of an alcohol. These cooperative effects are manifested in sometimes dramatic red shifts and IR intensity increases of symmetric O–H stretching modes of bonded water and alcohol functionalities, and in donor–acceptor interactions attributable to charge transfer among local bond/antibond orbitals. Electron-releasing field effects of methyl group substituents on ethene are also found to enhance the strength of the  $\pi$ H bond. The magnitude of cooperative  $\pi$ H- and normal  $\sigma$ H-type hydrogen-bonding effects in models presented here is similar to or exceeds that of the water dimer. Dynamic molecular clusters involving adventitious water molecules and the double bond of alkenes and AOHs, therefore, may have structural significance in assemblies of larger molecules, such as ceramides and sphingomyelin.

**Acknowledgment.** We acknowledge the National Eye Institute of the National Institutes of Health, which supported this research through grant EY11657. Computer time allocations were received from the National Computational Science Alliance under grants CHE98008N and CHE990012N and the Advanced Biomedical Computing Center of the Frederick Cancer Research and Development Center, National Institutes of Health.

## References and Notes

- Hannun, Y. A. *Science* **1996**, *274*, 1855.
- Bielawska, A.; Crane, H. M.; Liotta, D.; Obeid, L. M.; Hannun, Y. A. *J. Biol. Chem.* **1993**, *268*, 26226.
- Obeid, L. M.; Linardic, C. M.; Karolak, L. A.; Hannun, Y. A. *Science* **1993**, *259*, 1769.
- Li, Li; Tang, X.; Taylor, K. G.; DuPré, D. B.; Yappert, M. C. *Biophys. J.*, submitted for publication.
- Engdahl, A.; Nelander, B. *Chem. Phys. Lett.* **1985**, *113*, 49.
- Engdahl, A.; Nelander, B. *J. Phys. Chem.* **1986**, *90*, 4982.
- Peterson, K. I.; Klemperer, W. J. *Chem. Phys.* **1986**, *85*, 725.
- Andrews, A. M.; Kuczowski, R. L. *J. Chem. Phys.* **1993**, *98*, 791.
- Kim, K. S.; Tarakeshwar, P.; Lee, J. Y. *Chem. Rev.* **2000**, *100*, 4245.
- Del Bene, J. E. *Chem. Phys. Lett.* **1974**, *24*, 203.
- Hobza, P.; Zahradnik, R. *Chem. Rev.* **1988**, *88*, 87.
- Rovira, M. C.; Novoa, J. J.; Whangbo, M.-H.; Williams, J. M. *Chem. Phys.* **1995**, *200*, 319.
- Tarakeshwar, P.; Choi, H. S.; Lee, S. J.; Lee, J. Y.; Kim, K. S. *J. Chem. Phys.* **1999**, *111*, 5838.
- Tarakeshwar, P.; Kim, K. S.; Brutschy, B. *J. Chem. Phys.* **2000**, *112*, 1769.
- Reed, A. E.; Curtiss, L. A.; Weinhold, F. *Chem. Rev.* **1988**, *88*, 899.
- Weinhold, F. Natural Bond Orbital Methods. In *The Encyclopedia of Computational Chemistry*; Schleyer, P. v. R., Allinger, N. L., Clark, T., Gasteiger, J., Kollman, P. A., Schaefer III, H. F., Schreiner, P. R., Eds.; John Wiley & Sons: Chichester, 1998.
- Reed, A. E.; Weinhold, F.; Curtiss, L. A.; Pochatko, D. J. *J. Chem. Phys.* **1986**, *84*, 5687.
- Muller-Dethlefs, K.; Hobza, P. *Chem. Rev.* **2000**, *100*, 143.
- Tsuzuki, S.; Uchimaru, T.; Mikami, M.; Tanabe, K. *Chem. Phys. Lett.* **1996**, *252*, 206.
- Rablen, P. R.; Lockman, J. W.; Jorgensen, W. L. *J. Phys. Chem.* **1998**, *102*, 3782.
- Paizs, B.; Suhai, S. *J. Comput. Chem.* **1998**, *19*, 575.
- Kristyan, S.; Pulay, P. *Chem. Phys. Lett.* **1994**, *229*, 175.
- Frisch, M. J.; Del Bene, J. E.; Binkley, J. S.; Schaefer III, H. F. *J. Chem. Phys.* **1986**, *84*, 2279.
- Sorenson, J. M.; Gregory, J. K.; Clary, D. C. *J. Chem. Phys.* **1997**, *106*, 849.
- Frisch, M. J.; Trucks, G. W.; Schlegel, H. B.; Scuseria, G. E.; Robb, M. A.; Cheeseman, J. R.; Zakrzewski, V. G.; Montgomery, J. A., Jr.; Stratmann, R. E.; Burant, J. C.; Dapprich, S.; Millam, J. M.; Daniels, A. D.; Kudin, K. N.; Strain, M. C.; Farkas, O.; Tomasi, J.; Barone, V.; Cossi, M.; Cammi, R.; Mennucci, B.; Pomelli, C.; Adamo, C.; Clifford, S.; Ochterski, J.; Petersson, G. A.; Ayala, P. Y.; Cui, Q.; Morokuma, K.; Malick, D. K.; Rabuck, A. D.; Raghavachari, K.; Foresman, J. B.; Cioslowski, J.; Ortiz, J. V.; Stefanov, B. B.; Liu, G.; Liashenko, A.; Piskorz, P.; Komaromi,

I.; Gomperts, R.; Martin, R. L.; Fox, D. J.; Keith, T.; Al-Laham, M. A.; Peng, C. Y.; Nanayakkara, A.; Gonzalez, C.; Challacombe, M.; Gill, P. M. W.; Johnson, B.; Chen, W.; Wong, M. W.; Andres, J. L.; Head-Gordon, M.; Replogle, E. S.; Pople, J. A. *Gaussian 98*, Revision A.6; Gaussian, Inc.: Pittsburgh, PA, 1998.

(26) Boys, S. F.; Bernardi, R. *Mol. Phys.* **1970**, *19*, 553.

(27) Cook, D. B.; Sordo, J. A.; Sordo, T. L. *Int. J. Quantum Chem.* **1993**, *48*, 375.

(28) Weinhold, F. *NBO 4.0 Program Manual. Natural Bond Orbital Analysis Programs*; Theoretical Chemistry Institute and Department of Chemistry, University of Wisconsin: Madison, WI, 1996.

(29) Smit, M. B.; March, J. *March's Advanced Organic Chemistry. Reactions, Mechanisms, and Structure*, 5th ed.; J. Wiley & Sons: New York, 2001; p 16.

(30) Desiraju, G. R.; Steiner, T. *The Weak Hydrogen Bond in Structural Chemistry and Biology*; Oxford University Press: Oxford, 1999.

(31) Desiraju, G. R. *Acc. Chem. Res.* **1991**, *24*, 290.

(32) Steiner, T. *J. Chem. Soc., Chem. Commun.* **1997**, 727.

(33) Herrebout, W. A.; Everaert, G. P.; van der Veken, B. J.; Bulanin, M. O. *J. Chem. Phys.* **1997**, *107*, 8886.

(34) Everaert, G. P.; Herrebout, W. A.; van der Veken, B. J. *J. Mol. Struct.* **2000**, *550–551*, 399.